Translated from *Uspekhi Khimii* **61** 1805–1821 (1992) U.D.C. 541.2+546.65+546.66+546.799

# The anomalous stabilisation of the oxidation state 2+ of lanthanides and actinides

N B Mikheev, L N Auerman, I A Rumer, A N Kamenskaya, M Z Kazakevich
Institute of Physical Chemistry, Russian Academy of Sciences

ABSTRACT. The present review deals with the anomalous stabilisation of the oxidation state 2+ of a number of lanthanides and actinides. This stabilisation of the oxidation state 2+ is due to the lowering of the energy of a *d*-orbital as a result of crystal field splitting in the ligand field and *d*-electron participation in chemical bonding.

The bibliography contains 68 references.

## Contents

I. Introduction 990
II. Reduction of lanthanides and actinides to the oxidation state 2+ in chloride melts and determination of the standard oxidation potentials ($E^0_{M^{3+}/M^{2+}}$) 991
III. Hydration energies of divalent lanthanides 993
IV. Electron configuration of divalent lanthanides and actinides 994
V. Characteristics of the behaviour of divalent actinides in melts 995
VI. Stabilisation of the oxidation state 2+ of lanthanides and actinides in condensed clusters 995

## I. Introduction

The lanthanides (Ln) and actinides (An) are transition *f*-elements characterised by the gradual filling of the 4*f*- and 5*f*-orbitals with electrons. The lanthanides from praseodymium to ytterbium (except gadolinium) and the actinides from plutonium to nobelium (except curium) in the ground state of the neutral atoms have the same electron configuration $f^n s^2$, so that these elements should be divalent. In fact, however, for all the lanthanides and for the actinides from americium onwards, the most stable oxidation state is 3+ (except for No, for which the most stable oxidation state is 2+). Connick[1] was the first to emphasise that the predominant oxidation state 3+ for the lanthanides is not related to the ground state of the neutral atoms, but is determined purely by the quantitative ratio of the ionisation potentials $I_n$ and the chemical stabilisation (hydration, solvation, etc.) of the divalent and trivalent ions. A measure of the stability of the divalent state relative to the trivalent state in solution is provided by the oxidation potential $E^0_{M^{3+}/M^{2+}}$. For aqueous solutions, the standard oxidation potential can be expressed as follows:

$$E^0_{M^{3+}/M^{2+}} + 4.43 = \Delta G^\circ_{ion} + \Delta G^0_h(M^{3+}) - \Delta G^0_h(M^{2+}), \quad (1)$$

where 4.43 V is the standard electrode potential of the hydrogen electrode;[2] $\Delta G^\circ_{ion}$ the ionisation energy, calculated from the values of the third ionisation potential $I_3$; and $\Delta G^\circ_h(M^{2+})$ and $\Delta G^\circ_h(M^{3+})$ the hydration energies of the divalent and trivalent ions.

Nugent and co-workers[3] obtained theoretical estimates of $E^0_{M^{3+}/M^{2+}}$ for the lanthanides and actinides. The improved theory of electron spin-pairing due to Jørgenson[4] was used in the calculations, and a correlation was found between the energy of the first electron-transfer band in the spectra of trivalent Ln and An complexes on the one hand and the energy of the first *f*–*d*-transition band of divalent Ln and An and the corresponding oxidation potentials on the other. The observed relationships are semi-empirical. Because of the lack of experimental data, the relationship between the oxidation potentials and the spectral parameters was established from a small number of points (divalent Sm, Eu, and Yb for Ln, and Cf for An) (Tables 1 and 2).

**Table 1. Standard oxidation potentials of the $Ln^{3+}/Ln^{2+}$ couples ($E^0_{Ln^{3+}/Ln^{2+}}$) and *fd*-excitation energies of the free ions $Ln^{2+}$ ($E_{fd}$).**

| Ln | $E^0_{Ln^{3+}/Ln^{2+}}$, V | | | $E_{fd}$, eV (Ref.18) |
|---|---|---|---|---|
| | experimental (Ref.17) | calculated | | |
| | | (Ref.3) | (Ref.5) | |
| La | −2.94±0.08 | −3.1±0.2 | −3.8 | −0.891 |
| Ce | −2.92±0.08 | −3.2±0.2 | −3.5 | 0.406 |
| Pr | −2.84±0.06 | −2.7±0.2 | −3.0 | 1.593 |
| Nd | −2.62±0.05 | −2.6±0.2 | −2.8 | 1.892 |
| Pm | −2.44±0.06 | −2.6±0.2 | −2.5 | not known |
| Sm | −1.50±0.01 | −1.6±0.2 | −1.5 | 3.259 |
| Eu | −0.34±0.01 | −0.3±0.2 | −0.35 | 4.740 |
| Gd | −2.85±0.07 | −3.9±0.2 | −3.6 | −0.295 |
| Tb | −2.83±0.07 | −3.7±0.2 | −3.5 | 1.112 |
| Dy | −2.56±0.05 | −2.6±0.2 | −2.6 | not known |
| Ho | −2.79±0.06 | −2.9±0.2 | −2.9 | 2.236 |
| Er | −2.87±0.08 | −3.1±0.2 | −3.0 | 2.105 |
| Tm | −2.22±0.05 | −2.3±0.2 | −2.1 | 2.839 |
| Yb | −1.18±0.01 | −1.1±0.2 | −1.10 | 4.139 |

**Table 2.** Standard oxidation potentials of the $An^{3+}/An^{2+}$ couples ($E^0_{An^{3+}/An^{2+}}$) and *fd*-excitation energies of the free ions $An^{2+}$ ($E_{fd}$).

| An | $E^0_{An^{3+}/An^{2+}}$, V | | $E_{fd}$, eV (Ref.19) |
|---|---|---|---|
| | experimental (Ref.17) | calculated (Ref.3) | |
| Ac | not known | −4,9±0.2 | −3.434 |
| Th | not known | −4,9±0.2 | −1,872 |
| Pa | not known | −4,7±0.2 | −0.570 |
| U | −2.60±0.06 | −4,7±0.2 | 0.00 |
| Np | −2.83±0.07 | −4,7±0.2 | 0,508 |
| Pu | −2.79±0.07 | −3.5±0.2 | 1,699 |
| Am | −2.28±0.06 | −2,3±0.2 | 2.963 |
| Cm | −2.78±0.07 | −4.4±0.2 | 0,880 |
| Bk | −2.52±0.06 | −2.8±0.2 | 2.343 |
| Cf | −1.63±0.02 | −1.6±0.2 | 3.447 |
| Es | −1.45±0.02 | −1,3±0,2 | 3.744 |
| Fm | −1.18±0.02 | −1,1±0.2 | 3.992 |
| Md | −0.15±0.01 | 0,0±0.2 | 4.972 |
| No | +1.45±0.01 | +1,3±0.2 | 6,249 |

Another method for estimating $E^0_{M^{3+}/M^{2+}}$ for the lanthanides, used by Johnson,[5] is based on calculations from thermodynamic cycles. Experimental data for samarium, europium, and ytterbium were used in these calculations. The method is based on the assumption that the crystal lattice energies and the hydration energies of the ions change regularly with increase in atomic number and that the formation of a solid phase and the interaction of the ions with a solvent are not accompanied by a change in the number of *f*-electrons of the elements being considered. The calculated values of $E^0_{M^{3+}/M^{2+}}$ are given in Table 1.

The experimental data on the long familiar divalent state of samarium, europium, and ytterbium were supplemented in the late seventies by the preparation of the divalent state of many lanthanides (Pr,[6] Nd,[7] Pm,[8] Dy,[9] Ho,[10] Er,[11] Tm [12]) and actinides Am,[13] Bk,[14] Cf,[15] Es,[15] Fm[16]) and the determination of the standard oxidation potentials. The standard oxidation potentials of the $M^{3+}/M^{2+}$ couples were determined for these elements[17] (Tables 1 and 2).

Tables 1 and 2 show that for most Ln and An the experimental values of $E^0_{M^{3+}/M^{2+}}$ agree with the theoretical estimates. From the theoretically calculated $E^0_{M^{3+}/M^{2+}}$ values, the existence of the divalent states of the elements La, Ce, Gd, Tb, U, Np, Pu, and Cm should not be expected. In fact, Tables 1 and 2 show that the calculated standard oxidation potentials of the $M^{3+}/M^{2+}$ couples for Gd, Tb, U, Np, Pu, and Cm lie below −3 V. This oxidation potential (−3 V) is reached in the presence of the strongest known reducing agent—lithium—and a lower oxidation potential cannot be obtained in a condensed medium. Nevertheless, it has been established experimentally that these elements exist in the divalent state and that the standard oxidation potentials of their $M^{3+}/M^{2+}$ couples are appreciably higher than the theoretically calculated values (Tables 1 and 2).

It will be shown in the present work that the anomalous stabilisation of the oxidation state 2+ of these elements is due to the participation of *d*-orbitals in chemical bonding.

## II. Reduction of lanthanides and actinides to the oxidation state 2+ in chloride melts and determination of the standard oxidation potentials $E^0_{M^{3+}/M^{2+}}$

Since various actinides are available only in micro-quantities, the possibility of obtaining the *f*-elements in the oxidation state 2+ was investigated, and the values of $E^0_{M^{3+}/M^{2+}}$ determined, by cocrystallisation in the molten salt systems $(LnOCl)_{solid}-(LnCl_3-LnCl_2-SrCl_2)_{melt}$, where Ln = Pr, Nd, Sm, and Ho, the subscript solid denotes the solid phase, and the subscript melts denotes the melt. The oxide chlorides of all the actinides and lanthanides except thulium and ytterbium have the PbFCl crystal structure. Thus the cocrystallisation of micro-quantities of $Ln^{3+}$ and $An^{3+}$ will take place as a result of true isomorphism or isodimorphism. On the other hand, the divalent lanthanides and actinides resemble the alkaline earth elements, which do not form oxide chlorides. Thus $Ln^{2+}$ and $An^{2+}$ should not cocrystallise with solid LnOCl. Preliminary experiments confirmed this assumption. The entrainment of $Sr^{2+}$ and $Eu^{2+}$, and also $Cs^+$, by the solid phase did not exceed 0.1%. This resolved the question of the possible formation of anomalous mixed crystals of the reduced forms of the elements being studied with LnOCl. In these experiments, the potential of the system was determined by the ratio $Ln^{3+}/Ln^{2+}$ in the system. The use of the dichlorides of praseodymium, neodymium, samarium, and holmium made it possible to study the reduction of the lanthanides and actinides over a wide range of values of the oxidation potentials and, which is particularly important, at a low concentration of the elements being studied.

The method developed made it possible to determine the extent of the reduction of the *f*-element being studied and the difference between the standard oxidation potentials of the element being studied and the potential-determining element. For this it was necessary to know the equilibrium distribution of the micro-component between the solid phase LnOCl and the $LnCl_3-SrCl_2$ melt when both components are in the trivalent state:

$$D_0=[m^{3+}/m^{3+}]_{solid}[M^{3+}/M^{3+}]_{melt}, \quad (2)$$

where $D_0$ is the cocrystallisation coefficient, and m and M the quantities of the micro- and macro-components.

Since the micro-component in the reduced form does not cocrystallise with the solid phase, the distribution of the elements in the system containing the reducing agent, $(LnOCl)_{solid}-(LnCl_3-LnCl_2-SrCl_2)_{melt}$, will be described by the equation:

$$D_0=\left(\frac{m^{3+}}{M^{3+}}\right)_{solid}\left(\frac{M^{3+}+M^{2+}}{m^{3+}+m^{3-n}}\right)_{melt}, \quad (3)$$

where $n$ is the number of electrons involved in the reduction of the micro-element.

From Eqns. (2) and (3) and the Nernst equation, the equilibrium state in the system is described by the equation:

$$\ln\left[\frac{D_0}{D}\left(1+\frac{M^{2+}}{M^{3+}}\right)-1\right]=\frac{-\Delta E_{M-m}}{RT/nF}+n\cdot\ln\frac{M^{2+}}{M^{3+}}. \quad (4)$$

where $\Delta E_{M-m}=E_{M^{3+}/M^{2+}}-E_{m^{3+}/m^{(3-n)+}}$, and $n$ is the number of electrons in the reaction $m^{3+}+ne^-\rightarrow m^{(3-n)+}$. Thus if $D_0$ and $D$ are known for different ratios $M^{2+}/M^{3+}$, Eqn. (4) can be used to

determine the value of $n$, that is the number of electrons involved in the reduction of the ion of the micro-element, and $\Delta E_{M-m}$—the difference between the oxidation potentials of the couples $M^{3+}/M^{2+}$ (for the potential-determining macro-element) and $m^{3+}/m^{(3-n)+}$ (for the micro-element).

In a large number of experimental studies,[20-27] Eqn. (4) has been used to calculate $n$, that is the number of electrons involved in the reduction of $Ln^{3+}$ and $An^{3+}$. In all cases the value was practically equal to 1. This indicates that reduction takes place to the oxidation state 2+. This is illustrated for the reduction of $Pu^{3+}$ in Fig. 1. The result of the reduction is independent of the reducing agent used—$Pr^{2+}$ or $Nd^{2+}$. The authors cited[20-27] also calculated the difference between the oxidation potentials of the potential-determining elements and the elements being studied ($\Delta E_{M-m}$) (Table 3).

**Table 3. Differences between the oxidation potentials $\Delta E_{M-m} = E_{M^{3+}/M^{2+}} - E_{M^{3+}/M^{2+}}$ in chloride melts.[38]**

| M–m | $\Delta E_{M-m}$, V | M–m | $\Delta E_{M-m}$, V | M–m | $\Delta E_{M-m}$, V |
|---|---|---|---|---|---|
| Pr — La | +0.10±0.04 | Nd — Pm | −0.18±0.02 | Sm — Yb | −0.31±0.02 |
| Pr — Ce | +0.08±0.04 | Nd — Dy | −0.07±0.04 | Sm — Cf | +0.13±0.02 |
| Pr — Nd | −0.22±0.04 | Nd — Pu | +0.17±0.05 | Sm — Es | −0.05±0.01 |
| Pr — Gd | +0.01±0.03 | Nd — Am | −0.34±0.03 | Sm — Fm | −0.32±0.01 |
| Pr — Tb | −0.01±0.03 | Nd — Bk | −0.10±0.01 | Ho — Dy | −0.26±0.03 |
| Pr — Cm | −0.06±0.02 | | | Ho — Er | +0.08±0.06 |
| | | | | Ho — Tm | −0.38±0.15 |

**Table 4. Differences between the oxidation potentials of the $M^{3+}/M^{2+}$ couples in solutions and melts $\Delta E_{M_1-M_2}$, V.**

| Pair of elements | Water | | Ethanol | Acetonitrile | Chloride melts | |
|---|---|---|---|---|---|---|
| | electrochemistry (Refs. 3, 31) | thermochemistry (Ref.30) | cocrystallisation (Refs. 32,33) | electrochemistry (Refs. 36,37) | electrochemistry (Ref.35) | cocrystallisation (Ref.28) |
| Sm — Yb | −0.40±0.02; −0.32±0.01 | −0.36±0.08 | — | — | −0.354±0.007 | 0.31±0.02 |
| Sm — Eu | −1.20±0.03; −1.16±0.01 | −1.06±0.08 | — | −1.2 | −1.175±0.009 | — |
| Yb — Eu | −0.80±0.03; −0.84±0.01 | 0.70±0.08 | — | — | −0.821±0.008 | — |
| Nd — Dy | — | −0.06±0.08 | — | — | — | −0.07±0.04 |
| Yb — Fm | — | — | 0±0.02 | — | — | +0.01±0.02 |
| Sm — Es | — | — | 0±0.04 | — | — | −0.05±0.01 |
| Sm — Cf | — | — | 0.05±0.04 | +0.03 | — | +0.13±0.02 |

Thus the values of $\Delta E$ in chloride melts were determined experimentally (Table 3). Subsequent studies[28,29] established how the $\Delta E_{M_1-M_2}$ values change on going to other systems, in particular aqueous solutions (Table 4). Table 4 shows that the values of $\Delta E_{M_1-M_2}$ in chloride melts, aqueous solutions, and organic solutions are similar, irrespective of the nature of the liquid phase and temperature. On this basis, the known values of $E^0_{M^{3+}/M^{2+}}$ for various lanthanides and the experimentally determined values of $\Delta E_{M_1-M_2}$ were used to calculate the previously unknown standard oxidation potentials of $M^{3+}/M^{2+}$ couples for lanthanum, cerium, praseodymium, promethium, gadolinium, terbium, holmium, erbium, uranium, neptunium, plutonium, curium, and berkelium (Tables 1 and 2).

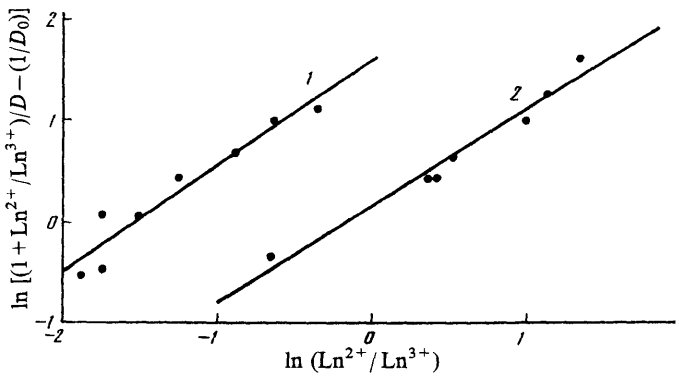



**Figure 1. Determination of the number of electrons involved in the reduction of $Pu^{3+}$ by $Pr^{2+}$ (1) and $Nd^{2+}$ (2).[22]**

The $M-MCl_3$ equilibrium diagrams for many $f$-elements show that the metallic lanthanides and actinides are soluble to a greater or lesser extent in their molten trichlorides. This phenomenon can be regarded as resulting from the reaction

$$M + 2MCl_3 \longrightarrow 3MCl_2.$$

Since in these systems the element is present in three oxidation states ($M^0$, $M^{2+}$, $M^{3+}$) in equilibrium, the following equation can be written for $T$ = 1173 K:

$$E_{M^{3+}/M^{2+}} + \frac{RT}{F}\ln\left[M^{3+}/M^{2+}\right] = E_{M^{3+}/M^0} + \frac{RT}{3F}\ln\left[M^{3+}\right]. \quad (5)$$

In this equation the values of $E_{M^{3+}/M^{2+}}$ and $E_{M^{3+}/M^0}$ in the molten salts at 1173 K are unknown. As shown in Table 4, however, $E_{M_1-M_2}$ is independent of temperature and the composition of the liquid phase. Thus the standard oxidation potential of the $M^{3+}/M^{2+}$ couple in the melt at 1173 K and the standard oxidation potential of the same couple in aqueous solution at 298 K $E^0_{M^{3+}/M^{2+}}$ will differ from one another by a constant quantity

$$E_{M^{3+}/M^{2+}} - E^0_{M^{3+}/M^{2+}} = a.$$

An analogous equation can be written for the oxidation potentials of the $M^{3+}/M^0$ couple:

$$E_{M^{3+}/M^0} - E^0_{M^{3+}/M^0} = b.$$

Replacing $E_{M^{3+}/M^{2+}}$ and $E_{M^{3+}/M^0}$ in Eqn. (5) by the corresponding values of the standard oxidation potentials gives:

$$E^0_{M^{3+}/M^{2+}} + \frac{1173R}{F}\ln\left[\frac{M^{2+}}{M^{3+}}\right] + a = E^0_{M^{3+}/M^0} + \frac{1173R}{3F}\ln\left[M^{3+}\right] + b, \quad (6)$$

from which it is possible to calculate the quantity $a - b$:

$$a - b = E_{M^{3+}/M^0} - E^0_{M^{3+}/M^{2+}} + \frac{1173R}{3F}\ln\left[M^{3+}\right] - \frac{1173R}{F}\ln\left[\frac{M^{3+}}{M^{2+}}\right]. \quad (7)$$

Table 5 gives the mole fractions $[M^{3+}]$ and $[M^{2+}]$ found from the solubility of the metal in the molten trichloride at 1173 K,[38] and also the standard oxidation potentials of the couples $M^{3+}/M^{2+}$ and the couples $M^{3+}/M^0$.[17,39,40] Table 5 also gives the values of $(a - b)$ for various lanthanides and actinides, calculated from the above data. Table 5 shows that the values of $(a - b)$ remain contant to within 45 mV.

**Table 5. Solubilities ($S$) of the metals in the molten trichlorides, the mole fraction $[M^{3+}]$ and $[M^{2+}]$ in the melts, the standard oxidation potentials of the couples $M^{3+}/M^{2+}$ and $M^{3+}/M^0$, and the calculated differences $a - b$.**

| M | $S$ M in $MCl_3$, mol% | $[M^{3+}]$ (Ref.38) | $[M^{2+}]$ (Ref.38) | $E^0_{M^{3+}/M^{2+}}$, V (Ref.17) | $E^0_{M^{3+}/M^0}$, V (Ref.39) | $a-b$, V (Ref.38) |
|---|---|---|---|---|---|---|
| La | 9 [41] | 0.73 | 0.27 | −2.94 | −2.36 | 0.47 |
| Ce | 9 [42] | 0.73 | 0.27 | −2.92 | −2.33 | 0.48 |
| Pr | 19 [42] | 0.43 | 0.57 | −2.84 | −2.34 | 0.50 |
| Nd | 30 [43] | 0.10 | 0.90 | −2.62 | −2.32 | 0.44 |
| Gd | 5 [44] | 0.85 | 0.15 | −2.85 | −2.28 | 0.39 |
| Ho | 20 [10] | 0.40 | 0.60 | −2.79 | −2.37 | 0.43 |
| Er | 7 [45] | 0.79 | 0.21 | −2.87 | −2.32 | 0.41 |
| Pu | 8 [46] | 0.76 | 0.24 | −2.59 | −2.02 | 0.44 |

average 0.44±0.04

The established correlation between the standard oxidation potentials of the couples $M^{3+}/M^{2+}$ and $M^{3+}/M^0$ and the solubility of the metal in the molten trichloride is observed irrespective of whether $M^{2+}$ is present in the melt in the configuration $f^n d^0 s^0$ or in the configuration $f^{n-1}d^1s^0$. Although the dichlorides of the lanthanides and the actinides in these two electronic states show different chemical properties, the differences between their free energies of reaction with the molten chlorides and with water are the same. All this made it possible to construct a single scale of standard oxidation potentials of the $M^{3+}/M^{2+}$ couples (Tables 1 and 2).

## III. Hydration energies of divalent lanthanides

Tables 1 and 2 show that for many of the elements, the experimentally determined values of the standard oxidation potentials of the $M^{3+}/M^{2+}$ couples[17] agree well with the calculated values.[3,5] In the lanthanide series, the exceptions are Gd and Tb. Calculations of the hydration energies of $Ln^{2+}$ from Eqn. (1)[47] were used to determine possible reasons for the anomalous behaviour of Gd and Tb. Fig. 2 (straight lines *1a* and *1b*) shows the dependence of the hydration energies of $Ln^{2+}$ on their atomic number. It follows from Fig. 2 that for most of the elements the hydration energies change linearly with increase in the atomic number ($Z$); this is due to the linear dependence of the ionic radius on the atomic number of the element (straight line *2* in Fig. 2).[48] La, Ce, Gd, and Tb, however, do not correspond to this relationship. $La^{2+}$ and $Gd^{2+}$ even as the free ions have the electron configuration $f^{n-1}d^1$. When the $Ln^{2+}$ ion is converted from the free state to the coordinated state, the $d$-state is stabilised by the splitting of the $d$-level in the crystal field of the ligands, and also by the increase in the covalent character of the chemical bonding with the ligands. The stabilisation energy of the $d$-level of $Ce^{2+}$ and $Tb^{2+}$ is greater than the $fd$-excitation energy of their free ions (0.406 eV and 1.112 eV respectively[18]), but on conversion into the coordinated state these elements will have the same electron configuration as the $La^{2+}$ and $Gd^{2+}$ ions. In this case it is convenient to calculate the hydration energies of $Gd^{2+}$ and $Tb^{2+}$ from Eqn. (1) using not the total ionisation energy but the energy of ionisation from the $d$-level, which can be calculated using the equation:

$$I_d = I_3 - E_{fd}, \quad (8)$$

where $I_d$ is the energy of ionisation from the $d$-level, and $E_{fd}$ the $fd$-excitation energy of the free doubly-charged ion.[18] Eqn. (1) then takes the form:

$$E^0_{M^{3+}/M^{2+}} + 4.43 = \Delta G^0_{ion}(d) + [\Delta G^0_h(M^{3+}) - \Delta G^0_h(M^{2+})], \quad (9)$$

where $\Delta G^0_{ion}(d)$ is the ionisation energy, calculated from the value of $I_d$.

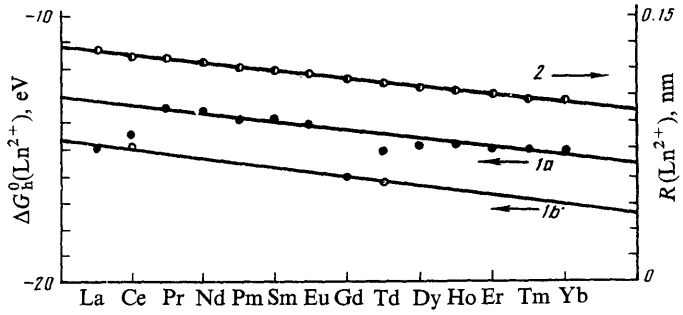



**Figure 2. Hydration energies [$\Delta G^0_h(Ln^{2+})$] (*1a*, *1b*) and ionic radii [$R(Ln^{2+})$] (*2*) of $Ln^{2+}$.[47,48]**

A feature of undoubted interest is that in this case the hydration energies for the neighbouring elements $La^{2+}$, $Ce^{2+}$ and $Gd^{2+}$, $Tb^{2+}$ have similar values, all of which lie on the straight line *1b* (Fig. 2), lying almost parallel to straight line *1a*. This indicates that the hydrated doubly-charged ions of La, Ce, Gd, and Tb have an

electron configuration involving *d*-electrons. Moreover, the fact that the two straight lines (*1a* and *1b* in Fig. 2) are almost parallel indicates a similarity in the changes in the ionic radius of $Ln^{2+}$ with change in atomic number in the two different electron configurations. The difference between the hydration energies of $Ln^{2+}$ in different electron configurations might be regarded as the stabilisation energy of the *d*-level. This is true, however, only if the ionic radii of $La^{2+}$, $Ce^{2+}$, $Gd^{2+}$, and $Tb^{2+}$ are independent of their electron configurations, and there is obviously no justification for this assumption. Moreover, the ionic radius of all the above elements in the $f^{n-1}d^1$ configuration should be greater than that expected if they had the electronic structure $f^nd^0$. Thus the stabilisation energy of the *d*-level for these elements will be greater than the differences between the hydration energies of the elements in the two different electron configurations (~1.6 eV for $La^{2+}$ and $Ce^{2+}$ and ~1.8 eV for $Gd^{2+}$ and $Tb^{2+}$). At the same time, the order of magnitude of the values obtained for the stabilisation is consistent with the energy of splitting of the *d*-level of La and Gd in a $CaF_2$ matrix, obtained by Johnson and Sandoe[49] (3 eV).

In addition to Ln, yttrium was also obtained in the divalent state, and the standard oxidation potential of the $Y^{3+}/Y^{2+}$ couple was determined (−2.82 V).[50] Yttrium is a typical *d*-element, whose doubly-charged ion has the electron configuration $4d^1$. It was therefore of interest to calculate the hydration energy of the $Y^{2+}$ cation using Eqn. (1). The hydration energy of the $Y^{2+}$ ion was found to lie on straight line *1b* (Fig. 2) in the range corresponding to the second half of the Ln family, confirming the electron configuration of $La^{2+}$, $Ce^{2+}$, $Gd^{2+}$, and $Tb^{2+}$.

## IV. Electron configuration of divalent lanthanides and actinides

The electron configuration of hydrated $Ln^{2+}$ ions was dealt with in a study[51] of the dependence of the standard oxidation potentials of the $M^{3+}/M^{2+}$ couples on the *fd*-excitation energy of the free doubly-charged ion. Figs. 3 and 4 give this relationship for the first and second halves of the Ln family, and show that the standard oxidation potential of the $M^{3+}/M^{2+}$ couple for most of the elements is linearly dependent on the *fd*-excitation energy (straight line *1*). This relationship can be explained if Eqn. (8) is used to express the ionisation energy $\Delta G^0_{ion}$ in terms of its two components. Eqn. (1) then becomes:

$$E^0_{M^{3+}/M^{2+}} + 4.43 = E_{fd} + [\Delta G^0_{ion}(d) + \Delta G^0_h(M^{3+}) - \Delta G^0_h(M^{2+})]. \quad (10)$$

The relationship $E^0_{M^{3+}/M^{2+}} = f(E_{fd})$ will obviously be linear if the quantity in square brackets does not depend or is linearly dependent on the *fd*-excitation energy. For elements such as La and Ce (Fig. 3) or Gd and Tb (Fig. 4), the standard oxidation potential of the $M^{3+}/M^{2+}$ couple for the two elements being compared is practically independent of the *fd*-excitation energy (straight line *2*). As noted above, this is related to the fact that in these elements in the coordinated state an electron is localised in a *d*-orbital. The anomalous position of $La^{2+}$, $Ce^{2+}$ and $Gd^{2+}$, $Tb^{2+}$ reflects their position in the sequence of change in the hydration energies of $Ln^{2+}$ with change in the atomic number (Fig. 2). Figs. 3 and 4 can be used to estimate the stabilisation energy of the *d*-level in aqueous solutions. It will obviously correspond to that *fd*-excitation energy of the free ion (the 4*f*-orbitals undergo practically no splitting in the crystal field of the ligands) which correspond to the point of intersection of straight lines *1* and *2* (Figs. 3 and 4). The values obtained using this approach for the stabilisation energy of the *d*-state are 1.6 eV for the first half of the lanthanide family, and 2.1 eV for the second, in good agreement with the values obtained from the hydration relationships (Fig. 2).

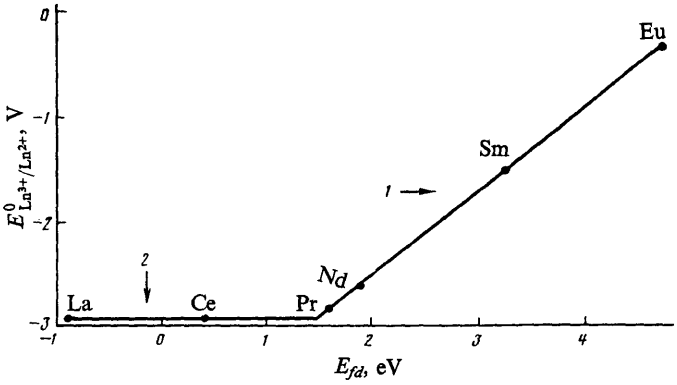



**Figure 3. Dependence of the standard oxidation potentials of the $Ln^{3+}/Ln^{2+}$ couples ($E^0_{Ln^{3+}/Ln^{2+}}$) on the *fd*-excitation energy of $Ln^{2+}$ ($E_{fd}$) for the first half of the lanthanide family.[47]**

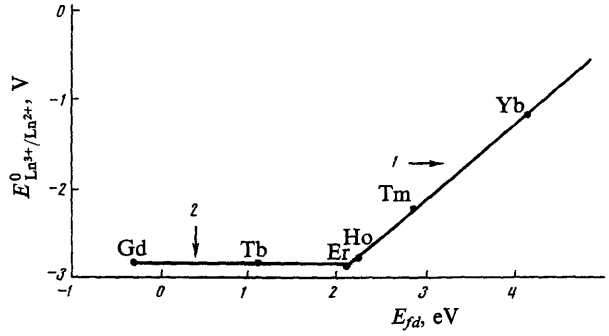



**Figure 4. Dependence of the standard oxidation potentials of the $Ln^{3+}/Ln^{2+}$ couples on the *fd*-excitation energy of $Ln^{2+}$ for the second half of the lanthanide family.[47]**

For An, the hydration energies of the $An^{2+}$ ions cannot be calculated using Eqn. (1) as in the case of Ln, since there are no experimental values of the third ionisation potentials and hydration energies of the $An^{3+}$ ions. The *fd*-excitation energies of the doubly-charged ions have been calculated for all An,[19] however, so that it has been possible to study the dependence of $E^0_{An^{3+}/An^{2+}}$ on the *fd*-excitation energies of the free doubly-charged ions (Fig. 5). Fig. 5 shows that the standard oxidation potential of the $M^{3+}/M^{2+}$ couple for U, Np, Pu, and Cm is independent of $E_{fd}$, as already observed for La, Ce, Gd, and Tb. Thus these elements of the An family in the divalent state apparently have an electron configuration with a *d*-electron. The stabilisation energy of the *d*-state for An is 2.1 eV, which coincides with the value obtained for the second half of the Ln family.

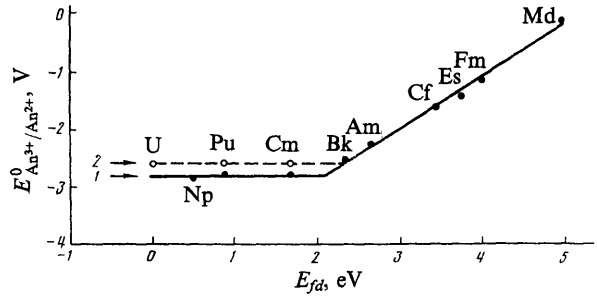



**Figure 5.** Dependence of the standard oxidation potentials of the $An^{3+}/An^{2+}$ couples ($E^0_{An^{3+}/An^{2+}}$) on the *fd*-excitation energy of $An^{2+}$ ($E_{fd}$) for the second half of the actinnide family.[47]

## V. Characteristics of the behaviour of divalent actinides in melts

An interesting feature is that the oxidation potential of the $Pu^{3+}/Pu^{2+}$ couple depends on the Pu concentration even in the micro-concentration range. With change in the Pu concentration from $\sim 10^{-4}$ mol% to $\sim 10^{-6}$ mol% the standard oxidation potential of the $Pu^{3+}/Pu^{2+}$ couple changes from $-2.59$ V to $-2.79$ V (Fig. 5). In addition, the standard oxidation potential of the $Cm^{3+}/Cm^{2+}$ couple in the presence of $\sim 10^{-4}$ mol% Pu also changes from $-2.78$ V to $-2.59$ V and coincides with the value for Pu at a concentration of $10^{-4}$ mol%. In addition to Cm, Pm was also added to the system; at the oxidation potential of the $Nd^{3+}/Nd^{2+}$ couple, Pm is reduced to the divalent state. In contrast to the case of Cm, the oxidation potential of $E^0_{Pm^{3+}/Pm^{2+}}$ remained unchanged in the presence of Pu.[52] Thus $Pu^{2+}$ is apparently able to form dimers or simple clusters. This distinguishes it from $Pm^{2+}$ and other divalent Ln and An with the electronic structure $f^n d^0$. The probability of this process evidently depends on the Pu concentration. In addition, $Cm^{2+}$ can also take part in the formation of clusters with Pu, and in this case its standard oxidation potential increases to the oxidation potential of the $Pu^{3+}/Pu^{2+}$ couple. The values of the standard $An^{3+}/An^{2+}$ oxidation potentials obtained for ponderable quantities of the elements of this family are given by straight lines *2* in Fig. 5. The "dimerisation" is an additional factor stabilising the oxidation state 2+, and was observed by us only for 5*f*-elements characterised in the divalent state by the participation of *d*-orbitals in chemical bonding.

For U there are no data on the standard oxidation potential of the $U^{3+}/U^{2+}$ couple in the micro-concentration range ($\sim 10^{-6}$ mol%), since the experiments on its reduction were carried out using the $^{233}U$ isotope at a concentration of $\sim 10^{-4}$ mol%.[53] The value of $E^0_{U^{3+}/U^{2+}}$ coincides with that of $E^0_{Pm^{3+}/Pm^{2+}}$ at the same concentration (Fig. 5). Thus uranium is apparently dimerised in the divalent state in the melt. This was confirmed by subsequent studies which showed that the oxidation potential of Cm increases to $-2.6$ V in the presence of ponderable quantities of uranium.

The behaviour of Np is of particular interest. Change in the Np concentration from $10^{-3}$ mol% to trace quantities has no influence on the value of $E^0_{Np^{3+}/Np^{2+}}$ (straight line *1* in Fig. 5). Thus $Np^{2+}$ does not form dimers in melts and in this respect differs from U, Pu, and Cm.[54]

The suggestion that dimers are formed was confirmed by studying the behaviour of $Pu^{2+}$ during the directed crystallisation of $NdBr_2$. In contrast to the case of $Am^{2+}$ and $Eu^{2+}$, for which the coefficient of cocrystallisation with $NdBr_2$ differs little from 1, the cocrystallisation coefficient of $Pu^{2+}$ is characterised by the presence of a maximum as the crystallisation of $NdBr_2$ proceeds (Fig. 6).[52,55] The authors cited explain the appearance of the maximum as follows. As the crystallisation tube moves from the hot zone of the melt to the cooled zone, decrease in temperature is accompanied by dimerisation. The resulting dimers cocrystallise with the $NdBr_2$ matrix with a high coefficient. Thus the crystallising $NdBr_2$ as it were "draws out" $Pu^{2+}$ from the melt. This is facilitated by the hindering of the back diffusion of dimerised plutonium into the hot zone of the melt. As a result, there is an appreciable decrease in the concentration of plutonium in the melt, so that the dimerisation stops and the cocrystallisation coefficient of Pu decreases in the final stage of the directed crystallisation. The directed-crystallisation experiments confirm the anomalous behaviour of $Pu^{2+}$ compared with $Am^{2+}$ and $Eu^{2+}$, resulting from the participation of *d*-orbitals of $Pu^{2+}$ in chemical bonding.

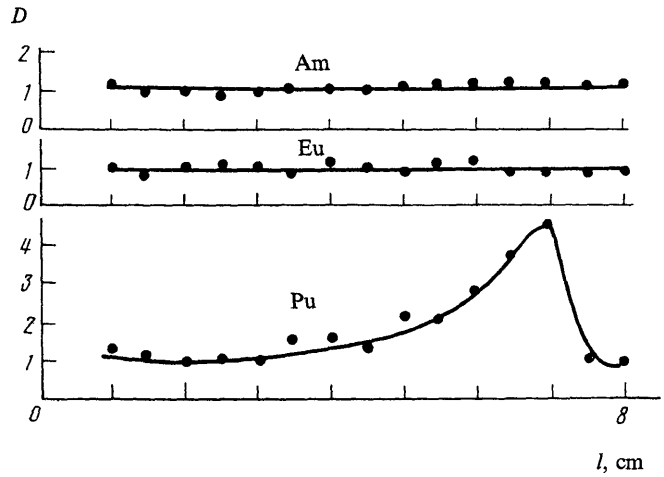



**Figure 6.** Distribution of $Pu^{2+}$, $Eu^{2+}$, and $Am^{2+}$ along the crystal (*l*) in the directed crystallisation of $NdBr_2$.[55]

## VI. Stabilisation of the oxidation state 2+ of lanthanides and actinides in condensed clusters

In recent years a number of condensed cluster compounds containing lanthanides having oxidation states from 1+ to 2.5+ have been synthesised.[56–61] It has been established[60] that the *d*-orbitals of the lanthanides take part in the formation of the M–M bond. The compound $Gd_2Cl_3$ was first obtained by the reaction of metallic Gd with molten Gd trichloride.[44] This cluster forms acicular crystals made up of chains of octahedra of gadolinium atoms joined to one another via shared edges. The mechanism of formation of the cluster has not been studied, however.

Two possible mechanisms of formation of the cluster have been proposed. The first is based on the disproportionation of gadolinium dichloride formed by the reaction of $Gd^0$ with $GdCl_3$:

$$Gd^0 + 2GdCl_3 \rightarrow 3GdCl_2 ,$$
$$\frac{3GdCl_2 \rightarrow Gd_2Cl_3 + GdCl_3}{Gd^0 + GdCl_3 \rightarrow Gd_2Cl_3} .$$

The second mechanism assumes reduction by metallic gadolinium sorbed on the cluster by a mechanism involving the primary sorption of the trivalent gadolinium ion:

$$Gd^0 \rightarrow Gd^{3+} + 3e^- ,$$
$$2GdCl_3 + 3e^- \rightarrow Gd_2Cl_3 + 3Cl^- ,$$
$$\frac{Gd^{3+} + 3Cl^- \rightarrow GdCl_3}{Gd^0 + CdCl_3 \rightarrow Gd_2Cl_3} .$$

The overall reaction is the same for both processes, so that it is difficult to establish the mechanism of formation of the cluster. At the same time it should be noted that a necessary condition for the first mechanism is the existence of divalent gadolinium. In this case, if a micro-component which is also reduced to the oxidation state 2+ and which like $Gd^{2+}$ has the electron configuration $f^{n-1}d^1$ is introduced into the system, then the extent of its cocrystallisation will be proportional to the fraction of this element in the divalent state. For the second mechanism, which assumes the participation of the trivalent form of the element in the cocrystallisation, the opposite relationship should be observed, that is decrease in the cocrystallisation with increase in the fraction of the reduced form of the cocrystallising element.

Equations have been derived,[62] describing the distribution of a micro-component between solid $Gd_2Cl_3$ and molten $GdCl_3$ for the two mechanisms, namely

$$\ln\frac{a}{a-x} = \frac{2(1+k)}{1+k\cdot\exp\left(\frac{\Delta E^0_{M-m}}{RT/F}\right)}\lambda_1\cdot\ln\frac{2b}{2b-y} , \qquad (11)$$

for the first mechanism and

$$\ln\frac{a}{a-x} = \frac{2(1+k)\cdot\exp\left(\frac{\Delta E^0_{M-m}}{RT/F}\right)}{1+k\cdot\exp\left(\frac{\Delta E^0_{M-m}}{RT/F}\right)}\lambda_2\cdot\ln\frac{2b}{2b-y} , \qquad (12)$$

for the second mechanism of formation of the cluster, where $a$ and $b$ are the initial concentrations of the micro-component and the macro-component in the $GdCl_3$ melt, $x$ and $y$ their concentrations in the cluster $Gd_2Cl_3$, $k$ the ratio of the concentrations $[Gd^{3+}]$ and $[Gd^{2+}]$ in the melt, and $\lambda$ the cocrystallisation coefficient.

It can be seen that if $\Delta E^0_{M-m} = 0$, both equations become

$$\ln\frac{a}{a-x} = 2\lambda\cdot\ln\frac{2b}{2b-y} , \qquad (13)$$

and in this case the mechanism of formation of the cluster cannot be determined. Thus to establish the mechanism of formation of the cluster it is necessary to determine the cocrystallisation coefficient $\lambda$ for elements which are chemically similar to Gd but which differ from gadolinium in the values of the standard oxidation potential of the $M^{3+}/M^{2+}$ couple. This requirement is satisfied by Np, Pu, and Cm (Table 2). Since we are considering actinides with similar ionic radii, the coefficients of their cocrystallisation with $Gd_2Cl_3$ should be close to one another.

Table 6 gives the values of the cocrystallisation coefficients $\lambda_1$ and $\lambda_2$ for Np, Pu, and Cm with $Gd_2Cl_3$, calculated from Eqns. (11) and (12), which describe respectively the first and second mechanisms of formation of the cluster.[62]

**Table 6.** Cocrystallisation coeffcients $\lambda_1$ and $\lambda_2$ for Np, Pu, and Cm with $Gd_2Cl_3$.[17]

| An | $E^0_{M^{3+}/M^{2+}}$, V | $\lambda_1$ | $\lambda_2$ |
|---|---|---|---|
| Np | -2.86 | 1.16 | 2.21 |
| Pu | -2.59 | 0.072 | 2.03 |
| Cm | -2.78 | 0.70 | 1.73 |

Table 6 shows that the values of $\lambda_1$, obtained assuming that the cocrystallisation takes place by the first mechanism, show poor agreement with one another. The situation is quite different if it is assumed that the second mechanism of cocrystallisation is correct. In this case the values of $\lambda_2$ for all three elements are close to one another, as expected for elements with similar properties It was therefore concluded[62] that the formation of the $Gd_2Cl_3$ cluster passes through a stage involving the sorption of the trivalent ion on the surface of the growing crystal and the subsequent reduction of $Ln^{3+}$ to the oxidation state 1.5+.

Subsequent studies showed that not every trivalent ion can enter the $Gd_2Cl_3$ matrix. For example, $Nd^{3+}$ and $Pu^{3+}$, which have similar ionic radii (0.0983 nm and 0.100 nm respectively) and practically identical standard oxidation potentials of the $M^{3+}/M^{2+}$ couples (−2.62 V and −2.59 V respectively), show completely different behaviour on cocrystallisation with the $Gd_2Cl_3$ cluster. Plutonium cocrystallises with $Gd_2Cl_3$, but $Nd^{2+}$ does not.[17] The explanation is that after sorption, the trivalent ion is reduced to the lower oxidation state by the "electron gas" in the $Gd_2Cl_2$ matrix. As can be seen from Fig. 5, Pu then acquires an electron configuration analogous to that of Gd, and takes part in the chemical bonding using its *d*-orbitals. In the case of Nd, the situation is quite different. As can be seen from Fig. 3, divalent neodymium does not have valence *d*-orbitals, and cannot take part in the construction of the $Gd_2Cl_3$ crystal lattice. Thus by studying the cocrystallisation with $Gd_2Cl_3$ it is possible to reach conclusions about the electron configuration of an *f*-element in the divalent state. Some elements which in the melt have the electron configuration $f^nd^0$, for example, Pr, Er, and Ho, cocrystallise with $Gd_2Cl_3$.[63,64] Figs. 3 and 4 show that Pr and Er lie at the intersection of straight lines *1* and *2*, corresponding to two different electron configurations of the ions in the divalent state, and the slight increase in the stabilisation energy of the *d*-level in the $Gd_2Cl_3$ crystal converts all of the above three elements into the $f^{n-1}d^1$ configuration. For Ho,

the *fd*-excitation energy is 0.13 eV greater than the stabilisation energy in melts. From this it follows that the stabilisation energy in the $Gd_2Cl_3$ matrix is approximately 0.13 eV greater than the stabilisation energy in the chloride melt. Our recent studies have shown that the same applies to the actinides. Thus berkelium cocrystallises with $Gd_2Cl_3$, whereas in the melt it has the configuration $[f^n d^0]^{2+}$. This indicates that for the actinides, the stabilisation energy of the *d*-level in $Gd_2Cl_3$ is 0.2 eV greater than that in the melt.

An important factor in cocrystallisation with the cluster is the ionic radius of the cocrystallising element. For example, in the series Pr–Ce–La the coefficient of cocrystallisation with the $Gd_2Cl_3$ cluster decreases from 0.5 for Pr to almost zero for La. The ionic radius of $La^{3+}$, which undergoes almost no cocrystallisation with $Gd_2Cl_3$, differs from that of $Gd^{3+}$ by about 10%. According to Mitscherlich, this difference between the ionic radii should lead to a sharp decrease in the miscibility of the elements in the solid phase, as observed in the cocrystallisation of Ce and more particularly La with $Gd_2Cl_3$.[63] The opposite dependence of the cocrystallisation coefficients on ionic radius is observed for the actinides, however, where $\lambda$ decreases in the series Pa–Np–Pu–Cm–Bk (Table 7). A possible explanation for this relationship and the comparatively high values of $\lambda$ for these elements may be that in addition to *d*-orbitals, the 5*f*-orbitals are also involved in chemical bonding.

**Table 7.** Cocrystallisation coefficients for actinides with the cluster $Gd_2Cl_3$

| An | Cocrystallisation coefficient $\lambda$ (Ref.17) | Ionic radius of $An^{3+}$, nm (Ref.65) |
|---|---|---|
| Pa | 3.00 | 0.104 |
| Np | 2.21 | 0.101 |
| Pu | 2.03 | 0.100 |
| Cm | 1.73 | 0.097 |
| Bk | 1.20 | 0.096 |

The study of the cocrystallisation of Ln and An with the $Gd_2Cl_3$ matrix has shown which elements of these families in the divalent state have a valence-electron configuration analogous to that of $Gd^{2+}$. Among the lanthanides these are La, Ce, Pr, Gd, Tb, Er, Ho, and Lu. To these can be added Y, which also has a *d*-electron in the divalent state. The actinides having an electron configuration with a *d*-electron are Pa, Np, Pu, Cm, and Bk.

Thus experimental data and information on the electronic structure of the free ions Ln and An show that a considerable number of elements of the *f*-series in the oxidation state 2+ are characterised by the participation of a *d*-electron in chemical bonding, leading to anomalous stabilisation of the oxidation state 2+, revealed by an increase in the oxidation potentials, an increase in the hydration energies, and the ability to form dimers and clusters.

* *
*

The anomalous stabilisation of lantanides and actinides in the oxidation state 2+ has made it possible to reduce La, Ce, Gd, Tb, U, Np, Pu, and Cm to the divalent state. The chemical properties of these ions are similar to those of divalent yttrium. Until now it has been considered that the divalent lanthanides and actinides are analogues of the alkaline earth elements. This is true for those elements, such as Eu, for which the *fd*-excitation energy is greater than the stabilisation energy of the *d*-level. For these elements the stability of the divalent state is linearly dependent on the *fd*-excitation energy. For those divalent elements which are analogues of divalent yttrium, the stability of the divalent state is determined not by the *fd*-excitation energy by by factors stabilising the *d*-level: the splitting of the *d*-level in the crystal field of the ligands, the covalent character of the bonds with the ligands, dimerisation, and possibly others.

The elements of a given family, Ln or An, may be analogues of elements of the *s*- or *d*-groups of Mendeleev's periodic system depending on the *f*–*d*-excitation energy.[66]

The observed constant value of the standard oxidation potential of the $An^{3+}/An^{2+}$ couples for U, Np, Pu, and Cm makes it possible to predict the value of this quantity for Ac and Pa (betwen −2.6 V and −2.9 V). There are no published data on the possible existence of Pa in the divalent state. For $Ac^{2+}$, the published values of its potential are −1.5 V[67] and above −1.6 V.[68] Both values are apparently too high.

Further studies will undoubtedly reveal many new and unusual features in the properties of *f*-elements showing anomalous stability of the oxidation state 2+.

## References


1. R E Connick *J. Chem. Soc. Suppl.*, 1949, (235)
2. E A Kanevskii *Dokl. Akad. Nauk SSSR*, 1981, **257** 926
3. L J Nugent, R D Baybarz, J L Burnett, J L Ryan *J. Phys. Chem.*, 1973, **77** 1528
4. C K Jørgensen *Chem. Phys. Lett.*, 1968, **2** 549
5. D A Johnson *J. Chem. Soc., Dalton Trans.*, 1974, 1671
6. L F Druding, J D Corbett, B N Ramsey *Inorg. Chem.*, 1963, **2** 869
7. L F Druding, J D Corbett *J. Am. Chem. Soc.*, 1959, **81** 5512
8. N B Mikheev, V I Spitsyn, L N Auerman, et al. *Radiokhimiya*, 1976, **18** 556
9. J D Corbett, B C MacCollum *Inorg. Chem.*, 1956, **5** 538
10. U Loechner, J D Corbett *Inorg. Chem.*, 1975, **14** 426
11. N B Mikheev, B G Korshunov, L N Auerman, et al. *Radiokhimiya*, 1981, **23** 624
12. P E Caro, J D Corbett *J. Less-Common Met.*, 1969, **18** 1
13. R D Baybarz, L B Asprey, C E Strouse, E Fukushima *J. Inorg. Nucl. Chem.*, 1972, **34** 3427
14. N B Mikheev, R A D'yachokva, V I Spitsyn *Dokl. Akad. Nauk SSSR*, 1979, **244** 109
15. N B Mikheev, V I Spitsyn, A N Kamenskaya, et al. *Radiokhimiya*, 1972, **14** 486
16. N B Mikheev, V I Spitsyn, B A Gvozdev, et al. *Dokl. Akad. Nauk SSSR*, 1971, **201** 1393
17. N B Mikheev, A N Kamenskaya *Coord. Chem. Rev.*, 1991, **109** 1
18. W C Martin, R Zalubas, L Hagan *Atomic Energy Levels—The Rare-Earth Elements*, NSRDS–NBS, 1978, No.60
19. K L Vander Sluis, L J Nugent *J. Opt. Soc. Am.*, 1974, **64** 687

20. N B Mikheev, R A D'yachkova, L N Auerman *Acta Chim. Acad. Sci. Hung.*, 1981, **108**(3) 249
21. V I Spitsyn, N B Mikheev, L N Auerman *Dokl. Akad. Nauk SSSR*, 1981, **261** 1154
22. N B Mikheev, L N Auerman, R A D'yachkova, I A Rumer *Izv. Akad. Nauk SSSR, Ser. Khim.*, 1982, 818
23. N B Mikheev, R A D'yachkova, L N Auerman, I A Rumer *Radiokhimiya*, 1982, **24** 112
24. N B Mikheev, L N Auerman, I A Rumer, R A D'yachkova *Radiokhimiya*, 1983, **25** 65
25. N B Mikheev, L N Auerman, I A Rumer *Zh. Neorg. Khim.*, 1983, **28**(5) 1329 [English translation in *Russ. J. Inorg. Chem.*, 1983(5)]
26. N B Mikheev, L N Auerman, I A Rumer *Radiokhimiya*, 1984, **26** 718
27. N B Mikheev, L N Auerman, I A Rumer, S A Kulyukhin, *Radiokhimiya*, 1984, **26** 415
28. N B Mikheev, L N Auerman, I A Rumer *Radiokhimiya*, 1984, **26** 646
29. N B Mikheev, L N Auerman, I A Rumer *Inorg. Chim. Acta*, 1985, **109** 217
30. L R Morss, M C McCue *Inorg. Chem.*, 1975, **14** 1624
31. D E Hobart, Ph. D. Thesis, University of Tennessee, Knoxville, 1981
32. N B Mikheev, V I Spitsyn, A N Kamenskaya, et al. *Radiokhimiya*, 1978, **20** 564
33. N B Mikheev, I A Rumer *Radiokhimiya*, 1972, **24** 492
34. C Musikas, R G Haire, J R Peterson *J. Inorg. Nucl. Chem.*, 1981, **43** 2935
35. K E Johnson, J R Mackenzie *J. Electrochem. Soc., Electrochem. Sci.*, 1969, **116** 1697
36. B F Myasoedov, Yu M Kulyako, I S Sklyarenko *Inorg. Nucl. Chem. Lett.*, 1972, **8** 433
37. H A Friedman, J R Stokely, R D Baybarz *Inorg. Nucl. Chem. Lett.*, 1972, **8** 433
38. N B Mikheev, L N Auerman, I A Rumer *Electrokhimiya*, 1987, **33** 638
39. V I Minkin (Editor) *Lantanoidy* (The Lanthanides), Izd. Rostov. Univ., Rostov-on-Don, 1980, p. 26
40. L L Borin, A I Karelin *Termodinamika Okislitel'no-vosstanovitel'nykh Protsessov v Tekhnologii Aktinidov* (The Thermodynamics of Redox Processes in the Technology of the Actinides), Atomizdat, Moscow, 1977, p. 207
41. D Brown *Halides of the Lanthanides and Actinides* (Translated into Russian), Atomizdat, Moscow, 1972, p. 161
42. H R Bronstein *J. Phys. Chem.*, 1969, **73** 1320
43. L F Druding, J D Corbett *J. Am. Chem. Soc.*, 1961, **83** 2462
44. J E Mee, J D Corbett *Inorg. Chem.*, 1965, **4** 88
45. J D Corbett, D L Pollard, J D Mee *Inorg. Chem.*, 1966, **5** 761
46. K W R Johnson, J A Leary *J. Inorg. Nucl. Chem.*, 1964, **26** 103
47. N B Mikheev, I L Rumer, L N Auerman *Radiokhimiya*, 1985, **27** 539
48. N B Mikheev *Radiokhimiya*, 1988, **30** 297
49. K E Johnson, J N Sandoe *J. Chem. Soc. A*, 1969, 1694
50. N B Mikheev, M Z Kazakevich, I L Rumer *Radiokhimiya*, 1990, **32** 40
51. N B Mikheev, I A Rumer, L N Auerman *Radiochem. Radioanal. Lett.*, 1983, **59** 317
52. N B Mikheev *Radiokhimiya*, 1988, **30** 16
53. N B Mikheev, E R Merts *Radiokhimiya*, 1990, **32** 1
54. N B Mikheev, I A Rumer, M Z Kazakevich *Radiokhimiya*, 1991, **33** 9
55. N B Mikheev, M Z Kazakevich I A Rumer *Radiokhimiya*, 1986, **28** 773
56. H J Mattausch, J B Hendricks, R Eger, et al. *Inorg. Chem.*, 1980, **19** 2128
57. A Simon, N Holzer, H J Mattausch *Z. Anorg. Allg. Chem.*, 1979, **456** 207
58. H J Mattausch, A Simon, N Holzer, R Eger *Z. Anorg. Allg. Chem.*, 1980, **466** 7
59. A Simon *Angew. Chem. Int. Ed. Engl.*, 1981, **20** 1
60. G Ebbinghaus, A Simon, A Griffith *Z. Naturforsch.*, 1982, **37a** 564
61. A Simon *J. Solid State Chem.*, 1985, **57** 2
62. N B Mikheev, I A Rumer, A N Kamenskaya, M Z Kazakevich *Radiokhimiya*, 1989, **31** 23
63. N B Mikheev, A N Kamenskaya, I A Rumer *Radiokhimiya*, 1991, **33** 10
64. N B Mikheev, A N Kamenskaya, I A Rumer *Radiokhimiya*, 1991, **33** 13
65. R D Shannon *Acta Crystallogr., Sect. A*, 1976, **32** 751
66. N B Mikheev *Naturwissenschaften*, 1989, **76** 107
67. F David *Radiochem. Radioanal. Lett.*, 1970, **5** 275
68. H Yamana, T Mitsugashira, Y Shiokawa, et al. *J. Radioanal. Chem.*, 1983, **76** 16

Received 8th May 1992